Available online at www.sciencedirect.com

SCIENCE DIRECT®

Journal of Organometallic Chemistry 689 (2004) 2707–2719

Journal of Organo metallic Chemistry

www.elsevier.com/locate/jorganchem

The reaction of *ortho*-halogenated aromatic aldazine ligands with $Fe_2(CO)_9$: symmetrical cleavage of the azine and carbon–halogen activation

Daniel Dönnecke, Kathi Halbauer, Wolfgang Imhof [*]

Institut für Anorganische und Analytische Chemie der Friedrich-Schiller-Universität Jena, August-Bebel-Str. 2, 07743 Jena, Germany

Received 4 March 2004; accepted 30 April 2004

Abstract

Azine ligands derived from hydrazine and benzaldehyde derivatives bearing halogen substituents in *ortho*-position with respect to the carbonyl function upon treatment with $Fe_2(CO)_9$ show two typical reaction principles. One is the symmetrical cleavage of the N–N bond of the azine to yield either di- or trinuclear iron carbonyl compounds $[Fe_2(CO)_6(\mu_2\text{-}N{=}CHR)_2]$ and $[Fe_3(CO)_9(\mu_2\text{-}N{=}CHR)(\mu_2\text{-}\eta^2\text{-}N{=}CHR)]$ each showing two arylidenimido moieties. In addition, a trinuclear iron carbonyl cluster compound exhibiting a tetrahedral Fe_3N cluster core is isolated. The cluster shows only one half of the former azine ligand. It is a ionic compound of the general formula $[Fe_3(CO)_9(\mu_3\text{-}\eta^2\text{-}N{=}CHR)]Na \times H_2O$. This trinuclear cluster compound is quantitatively converted into $[Fe_3(CO)_9(\mu_2\text{-}H)(\mu_3\text{-}\eta^2\text{-}N{=}CHR)]$ upon treatment with phosphorous acid. Most interestingly, we were also able to isolate two types of compounds in which an activation of one of the carbon halogen bonds in *ortho*-position with respect to the imine functions of the azine has occured in terms of an *ortho*-metallation reaction. In $[Fe_2(CO)_6(\mu_3\text{-}\eta^2\text{-}\overline{C{=}C(F)\text{-}C(H){=}C(H)\text{-}C(H){=}C}\text{-}CH_2\text{-}N\text{-}N{=}CHR)]$ the N–N bond of the azine is still preserved, whereas in $[Fe_3(CO)_9(\mu_3\text{-}\eta^3\text{-}N{=}CHR)]$ again only one half of the former azine ligand is coordinated in an arylidenimido fashion. In both types of compounds one additional iron carbon bond is present due to the activation of an aromatic carbon halogen bond. The reaction of iron carbonyls with 2,6-difluorobenzonitrile produces $[Fe_3(CO)_9(\mu_3\text{-}\eta^2\text{-}N{\equiv}CR)]$ as the sole product. All new iron carbonyl compounds are characterized by means of X-ray crystallography.

Keywords: C–F activation; C–Cl activation; Iron; Cluster compounds; X-ray analyses

1. Introduction

The activation of carbon halogen bonds and in this context especially of carbon fluorine bonds has attracted the interest of several research groups mainly for two reasons. First of all perfluorinated organic compounds may be functionalized that way to produce new fluorinated compounds [1]. This is an attractive goal since the properties of fluorinated organic compounds usually differ compared to those of the corresponding hydrocarbon derivatives [2]. Secondly, the transition metal induced activation of carbon halogen bonds might lead to strategies allowing the efficient degradation of environmentally critical halogenated hydrocarbons.

Since transition metal compounds have successfully been used in stoichiometric and catalytic activations of C–C ($\sim$350 kJ mol^{-1}) and C–H ($\sim$410 kJ mol^{-1}) bonds, the question arose whether transition metal compounds could also activate C–F bonds. Mechanistical studies on C–F activation reactions have revealed different activation mechanisms depending on the electronic structure

---

[*] Corresponding author. Tel.: +49-3641-948144; fax: +49-3641-948102.

E-mail address: cwi@rz.uni-jena.de (W. Imhof).

0022-328X/$ - see front matter © 2004 Elsevier B.V. All rights reserved.
doi:10.1016/j.jorganchem.2004.04.049

of the transition metal as well as additional ligands being present in the system. Quite a lot of reactions take place with titanium or zirconium compounds with hydride ligands present [3]. The reaction then is believed to take place via a transition state typical for σ-bond metathesis reactions in the case of fluoroaromatics. A similar transition state might also work in the reaction of $[OsH_6(P^iPr_3)_2]$, compound being able to activate C–H as well as C–F bonds [4]. Most of the stoichiometric C–F activation reactions reported in the literature are realized by treatment of the corresponding fluorinated organic compounds with transition metal complexes of late transition metals. Especially nickel [5], rhodium [6], platinum [7] and rhenium [8] have been commonly used for this purpose. In the reaction of fluoroaromatic compounds there is experimental evidence for two competing pathways. On one hand, the formation of tight ion-pairs by a complete electron transfer due to the high electron affinity of fluorine is discussed [9]. On the other hand, concerted mechanisms with an intermediate η^2-coordination of the C–F bond in the transition state have been made plausible by investigations of the kinetics as well as by the regioselectivity of C–F activation of heteroaromatic fluorocarbons, although in the latter case a pre-coordination via the heteroatom cannot be ruled out completely [1e]. In the case of aromatic hydrocarbons a η^2-coordination of the aromatic system has been identified in intermediates of C–F activation reactions and the compounds have been structurally characterized [5d,10]. Examples of catalytic reactions proceeding via C–F activation steps are very rare, the most prominent one being the synthesis of C_6F_5H from C_6F_6 catalyzed by rhodium compounds [11]. Of course catalytical activation of carbon halogen bonds plays a crucial role in dehalogenation reactions in vivo by reductive dehalogenases [12].

The above mentioned details are highly related to the synthetic problems and mechanistical discussions on transition metal induced C–H activation reactions. In the last years we were working on C–H activation reactions of aromatic imines both in stoichiometric [13] and catalytic reactions [14]. In this context we found that reactions of the imines with $Fe_2(CO)_9$ lead to iron carbonyl compounds that may serve as model compounds for the initiating reaction steps in catalytic reactions of the same imines as substrates in the presence of $Ru_3(CO)_{12}$ as the precatalyst. In order to develop reactions of improved atom economy we looked at the chemistry of $Fe_2(CO)_9$ towards aromatic azines, in which two α,β-unsaturated imine moieties are directly linked. We found that this reaction follows two major pathways. One of them is C–H activation in *ortho*-position with respect to the exocyclic imine substituent, the other one is a metal induced disproportionation of the azine into a primary imine and a nitrile. The same reaction principles are also observed in catalytic C–C coupling reactions starting from the same substrates [15].

Herein we report the chemistry of aromatic azines derived from benzaldehyde derivatives with halogen substituents in *ortho*-position with respect to the carbonyl function. In analogy to the corresponding hydrocarbons the reaction with $Fe_2(CO)_9$ proceeds via cleavage of the central N–N bond of the ligand or via the activation of a carbon halogen bond in terms of an *ortho*-metallation reaction. The latter reactivity is somehow related to the reactions of (perfluorovinyl)diiron complexes with amines, hydrazines, thiols or alcohols with the activation of a vinylic carbon fluorine bond as the initial step of the reaction [16]. The activation of carbon chlorine bonds has been reported during the reaction of $Fe_2(CO)_9$ with chlorobutadienes [17].

2. Results and discussion

The azines **1a** and **1b** are easily prepared by reacting hydrazine hydrate with two equivalents of 2,6-dichloro-benzaldehyde or 2,6-difluoro-benzaldehyde, respectively. Scheme 1 shows the reaction of **1a** with $Fe_2(CO)_9$ in heptane as the solvent. Chromatographic workup of the reaction mixture shows, that it consists mainly of unreacted **1a** and $Fe_3(CO)_{12}$. In addition, the trinuclear cluster compound **2a** is produced in small yields. The molecular structure of **2a** is presented in Fig. 1 together with the most important bond lengths and angles. The cluster is best described as a Fe_3N tetrahedron, in which the nitrogen atom is part of an arylidenimido moiety. The imine C–N double bond coordinates to Fe1 in a side-on fashion. In addition, there is a carbon iron bond (Fe2–C7) showing that the chlorine atom, that was situated at C7 in the starting compound, has been removed by an iron mediated activation of the corresponding

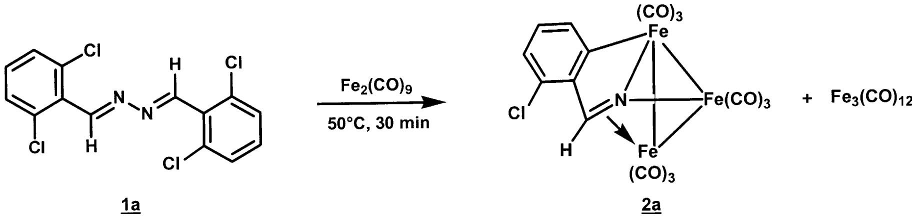

Scheme 1.

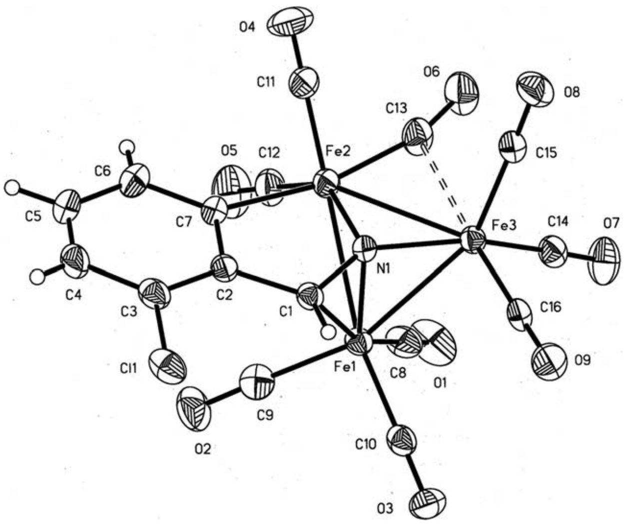

Fig. 1. Molecular structure of **2a**. Selected bond lengths (pm) and angles (°): Fe1–Fe2 257.63(8), Fe1–Fe3 253.11 (9), Fe2–Fe3 263.7(1), Fe1–N1 194.8(3), Fe2–N1 185.5(3), Fe3–N1 182.5(3), Fe1–C1 223.3(4), Fe2–C7 202.9(4), C1–N1 134.5(4), Fe2–Fe1–Fe3 62.16(2), Fe1–Fe2–Fe3 58.08(2), Fe2–Fe3–Fe1 59.76(3), Fe2–Fe1–N1 45.86(8), Fe3–Fe1–N1 45.83(8), Fe1–Fe2–N1 48.91(9), Fe3–Fe2–N1 43.77(9), Fe1–Fe3–N1 49.98(9), Fe2–Fe3–N1 44.70(9), Fe1–N1–Fe2 85.2(1), Fe1–N1–Fe3 84.2(1), Fe2–N1–Fe3 91.5(1), C1–N1–Fe1 83.2(2), C1–N1–Fe2 119.9(2), C1–N1–Fe3 144.8(3), N1–Fe2–C7 81.2(2), Fe2–C7–C2 111.1(3), C7–C2–C1 113.6(3), C2–C1–N1 111.6(3).

carbon chlorine bond. One of the CO ligands at Fe2 shows a semi-bridging coordination mode towards Fe3 leading to a slightly enhanced iron carbon bond length Fe2–C13 compared to the corresponding bond lengths of terminal CO ligands and a bond angle of Fe2–C13–O6 of 164.0°. Similar trinuclear iron carbonyl cluster compounds with a bridging hydride ligand instead of a formal carbanion have been observed from the reaction of carbonylferrates with nitriles in the presence of a proton source and from the iron induced disproportionation reaction of aromatic azines [15,16]. So we think that the formation of **2a** is also due to a disproportionation of **1a** into a primary imine and a nitrile and **2a** being the product of the reaction of the nitrile with $Fe_2(CO)_9$. Recently, the rhodium induced cleavage of an azine into a nitrile and a imine has been reported and the molecular structure of the corresponding nitrile complex was determined [19].

The fluoro compound **1b** turns out to be much more reactive when treated with $Fe_2(CO)_9$ compared to **1a**. Unfortunately, the reaction of **1b** is very unselective and we were able to identify and characterize five iron carbonyl cluster compounds, which are shown in Schemes 2 and 3. Scheme 2 shows the products **2b** and **3** which are produced via the activation of a carbon fluorine bond in **1a**. The trinuclear iron carbonyl cluster **2b**

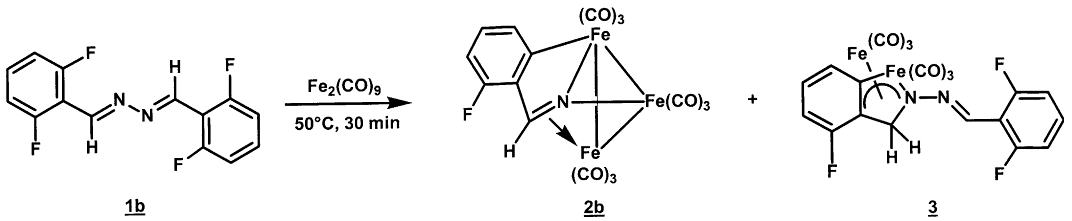

Scheme 2.

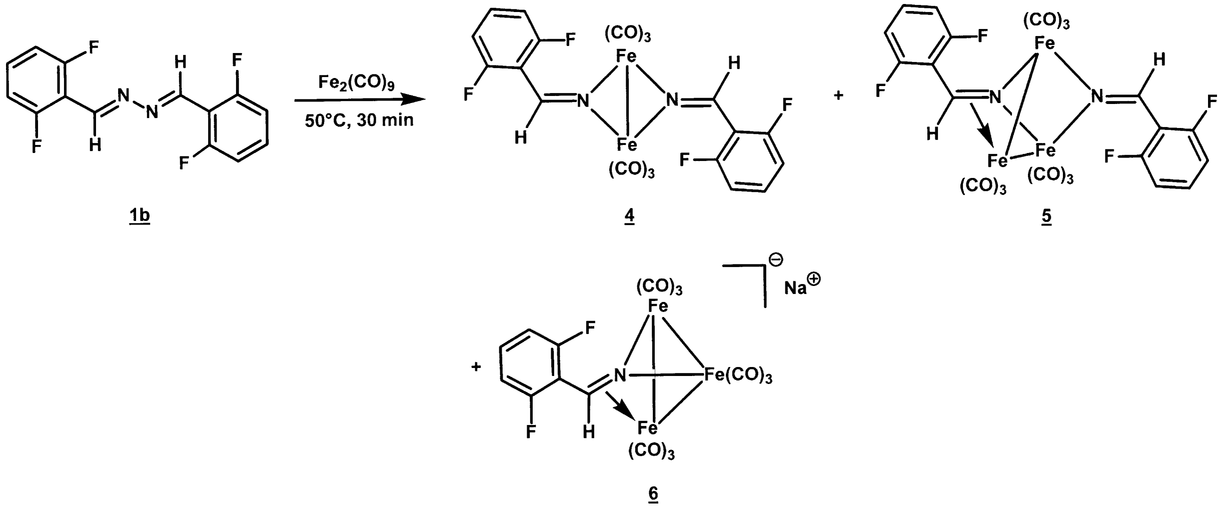

Scheme 3.

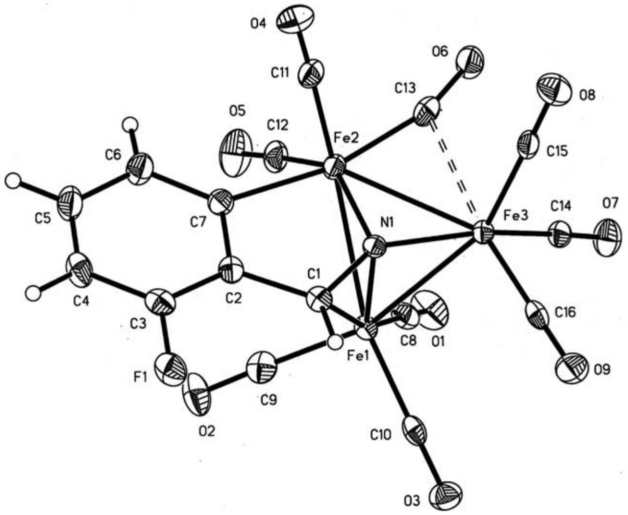

Fig. 2. Molecular structure of **2b**. Selected bond lengths (pm) and angles (°): Fe1–Fe2 258.01(5), Fe1–Fe3 252.22(4), Fe2–Fe3 261.92(4), Fe1–N1 194.9(2), Fe2–N1 186.0(2), Fe3–N1 183.2(2), Fe1–C1 223.6(2), Fe2–C7 202.6(2), C1–N1 133.9(3), Fe2–Fe1–Fe3 61.76(1), Fe1–Fe2–Fe3 58.03(1), Fe2–Fe3–Fe1 60.21(1), Fe2–Fe1–N1 45.91(5), Fe3–Fe1–N1 46.19(6), Fe1–Fe2–N1 48.85(5), Fe3–Fe2–N1 44.37(6), Fe1–Fe3–N1 50.18(6), Fe2–Fe3–N1 45.23(6), Fe1–N1–Fe2 85.25(7), Fe1–N1–Fe3 83.62(8), Fe2–N1–Fe3 90.40(9), C1–N1–Fe1 83.5(1), C1–N1–Fe2 119.7(2), C1–N1–Fe3 145.9(2), N1–Fe2–C7 81.66(9), Fe2–C7–C2 111.0(2), C7–C2–C1 113.5(2), C2–C1–N1 112.1(2).

is an isomer of **2a** with a fluoro substituent instead of a chloro group. The molecular structure is shown in Fig. 2 together with selected bond lengths and angles. **2b** shows the same bonding modes of the ligands at the trinuclear cluster core as they have been discussed for **2a** and the bond lengths and angles are nearly identical. As it can be seen from Table 1, in which all crystal and intensity data of the structural analyses are summarized, **2a** and **2b** are almost isostructural. Compound **3** is a dinuclear iron complex in which the central N–N bond of the azine ligand is still preserved. The molecular structure of **3** is depicted in Fig. 3, the most important bond lengths and angles may be found in the Figure Caption. One of the *ortho*-fluorinated aromatic moieties also shows a C–F activation reaction and a new carbon iron bond instead (Fe1–C1). To our surprise there is an additional hydrogen atom at C7 thus building up a methylene group at this position. The resulting aza-ferra-cyclopentadiene system is apically coordinated by the second $Fe(CO)_3$ moiety. This coordination mode has quite frequently been observed in the reaction of aromatic imines or azines, respectively [13,15]. In this cases, the formation of the dinuclear product clusters has been rationalized by the reaction sequence of a C–H activation in *ortho*-position with respect to the exocyclic imine function followed by an intramolecular hydrogen transfer towards the former imine nitrogen atom [13]. So we very carefully looked at the substrates 2,6-difluoro-benzaldehyde and **1b**, if there was any impurity by monosubstituted compounds and were able to exclude this possibility. So the additional hydrogen atom at C7 in **3** presumably is also due to the disproportionation of the azine into an imine and a nitrile, because in this reaction one of the imine carbon hydrogen bonds has to be broken.

Scheme 3 shows all iron carbonyl compounds from the reaction of **1b** with $Fe_2(CO)_9$, which are formed via the cleavage of the central N–N bond of the ligand. The molecular structure of **4** is shown in Fig. 4 together with the most important bond lengths and angles. **4** is a dinuclear iron carbonyl compound, which is best described as a bis-(μ-iminato)-complex. Compounds of this type are quite commonly obtained from the reaction of aldazines or ketazines with iron carbonyls [20]. The typical features for these complexes are the short C–N bond lengths of 123.9(9) and 125.2(9) pm, respectively, clearly indicating double bonds as well as the butterfly-structure of the Fe_2N_2 moiety with an angle of 79.4° between the two Fe_2N planes. In principle compounds like **4** may be obtained as *syn*- or *anti*-isomers due to the different substituents at the iminato carbon atoms. ^1H NMR spectroscopy shows the *syn*- and the *anti*-isomer in 40:60 ratio. Crystals suitable for X-ray diffraction experiments could be obtained for the *anti*-isomer only (Fig. 4).

Since crystals of compound **5** were of unsufficient quality, we were only able to obtain a structural motif of **5**, which is shown in Fig. 5. Bond lengths and angles will not be discussed. Compound **5** is a trinuclear iron carbonyl cluster being closely related to **4**, from which it is most probably produced by the reaction with an additional $Fe(CO)_3$ fragment. The molecule consists of a nearly planar Fe_2N_2 ring with two iminato units bridging the iron atoms. In contrast to **4** there is no iron–iron bond between the iron atoms of the Fe_2N_2 ring in **5**. One of the carbon nitrogen double bonds of the iminato moieties is coordinated to the third $Fe(CO)_3$ group in a side-on fashion. This iron atom (Fe1) is bound to both iron atoms of the Fe_2N_2 ring. So in summary the cluster core consists of an open triangle of iron atoms, one μ_3-nitrogen atom (N1) and one nitrogen atom (N2) bridging only two iron centers. It is obvious, that **5** is of much lower symmetry when compared to **4** leading to two sets of resonances for the iminato groups and their aromatic substituents in the NMR spectra. In addition, two isomers of **5** are observed according to the *syn*- and *anti*-isomers of **4** from which **5** most probably is produced (cf. Section 3).

Fig. 6 shows the molecular structure of the cluster anion in **6** together with selected bond lengths and angles. **6** was obtained as it is sodium salt together with two equivalents of water per ion pair. During the chromatographic workup of the product mixture of the reaction of **1b** with $Fe_2(CO)_9$ we recognized, that there was a compound which could neither be eluted with pure

Table 1
Crystal and intensity data for **2a**, **2b**, **3**, **4**, **6–8**

	2a	**2b**	**3**	**4**	**6**	**7**	**8**
Formula	$C_{16}H_4NO_9ClFe_3$	$C_{16}H_4NO_9FFe_3$	$C_{16}H_9N_2O_6F_3Fe_2$	$C_{16}H_8N_2O_6F_4Fe_2$	$[C_{16}H_4NO_9F_2Fe_3]Na \times H_2O$	$C_{16}H_5NO_9F_2Fe_3$	$C_{16}H_3NO_9F_2Fe_3$
Molecular weight ($g mol^{-1}$)	557.20	540.75	541.99	559.98	600.07	560.76	558.74
Radiation	Mo Kα	Mo Kα	Mo Kα	Mo Kα	Mo Kα	Mo Kα	Mo Kα
Monochromator	Graphite	Graphite	Graphite	Graphite	Graphite	Graphite	Graphite
Temperature (K)	183	183	183	183	183	183	183
Crystal color	Red	Orange	Red	Orange	Red	Red	Red
Crystal size	0.3×0.3×0.02	0.1×0.04×0.03	0.2×0.2×0.01	0.1×0.1×0.06	0.4×0.2×0.2	0.3×0.1×0.01	0.03×0.03×0.02
a (Å)	12.9019(6)	12.6823(4)	8.626(3)	7.3162(4)	15.9274(4)	15.225(2)	14.3458(2)
b (Å)	1 3.059(1)	13.0148(6)	9.407(3)	12.216(1)	13.3940(5)	7.065(2) 4	16.0535(3)
c (Å)	11.632(1)	11.3316(6)	13.408(4)	12.812(1)	20.4140(6)	18.183(3)	16.4510(4)
α (°)	90	90	73.30(2)	82.19(4)	90	90	90
β (°)	101.25(5)	103.952(3)	80.05(2)	77.21(4)	108.169(2)	101.62(1)	90
γ (°)	90	90	79.87(1)	73.60(4)	90	90	90
Volume ($Å^3$)	1922.1(3)	1815.2(1)	1017.2(5)	1068.0(2)	4137.8(2)	1911.1(6)	3788.7(1)
Z	4	4	2	2	8	4	8
F(000)	1096	1064	540	556	2368	1104	2192
ρ_{calc} ($g cm^{-3}$)	1.925	1.979	1.770	1.741	1.929	1.949	1.959
Crystal system	Monoclinic	Monoclinic	Triclinic	Triclinic	Monoclinic	Monoclinic	Orthorhombic
Space group	$P2_1/c$	$P2_1/c$	$P\bar{1}$	$P\bar{1}$	$P2_1/n$	$P2_1/c$	*Pbca*
Absorption coefficient (mm^{-1})	2.424	2.428	1.495	1.434	2.170	2.318	2.338
θ limit (°)	$2.24 < \theta < 27.44$	$2.28 < \theta < 27.48$	$2.28 < \theta < 27.63$	$2.96 < \theta < 27.54$	$1.43 < \theta < 27.50$	$1.37 < \theta < 27.56$	$2.27 < \theta < 27.47$
Scan mode	ω-scan	ω-scan	ω-scan	ω-scan	ω-scan	ω-scan	ω-scan
Reflections measured	6403	7281	6493	7795	17154	5592	8116
Independent reflections	4311	4151	4210	4767	9212	4220	4322
R_{int}	0.0450	0.0307	0.0739	0.0567	0.0551	0.0896	0.0337
Reflections observed ($F_0^2 > 2\sigma(F_0^2)$)	2885	3221	2489	3346	9206	1889	3297
No. of parameters	287	287	309	311	619	284	292
Goodness-of-fit	0.991	1.004	1.049	1.200	1.026	1.011	1.007
R_1	0.0439	0.0315	0.0772	0.1179	0.0504	0.0841	0.0333
wR_2	0.0814	0.0636	0.1717	0.3027	0.0935	0.1676	0.0758
Final diffraction map electron density peak ($e Å^{-3}$)	0.421	0.459	0.883	5.365	0.433	1.016	0.340

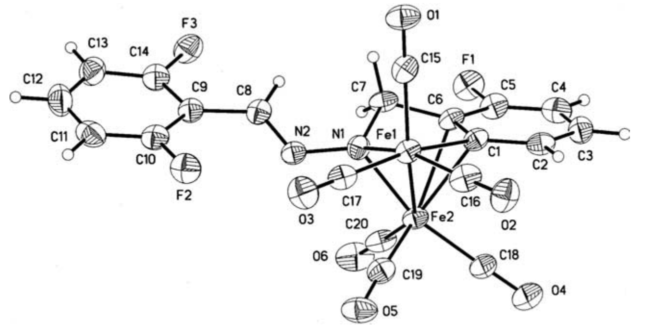

Fig. 3. Molecular structure of **3**. Selected bond lengths (pm) and angles (°): Fe1–Fe2 244.2(1), Fe1–N1 196.4(6), Fe1–C1 200.4(6), Fe2–N1 195.4(5), Fe2–C1 218.8(6), Fe2–C6 231.6(6), C1–C6 142.1(9), C6–C7 149.5(9), N1–C7 149.5(8), N1–N2 139.4(8), N2–C8 129.7(9), C8–C9 145.0(1), N1–Fe1-C1 78.9(2), Fe1–C1–C6 111.9(5), C1–C6–C7 117.1(5), C6–C7–N1 99.3(5), C7–N1–Fe1 113.7(4), Fe1–Fe2–N1 51.6(2), N1–Fe1–Fe2 51.3(2), Fe1–N1–Fe2 77.1(2), Fe1–Fe2–C1 50.9(2), Fe2–Fe1–C1 58.0(2), Fe1–C1–Fe2 71.1(2), Fe1–Fe2–C6 73.8(1), N1–F2–C1 74.8(2), N1–Fe2–C6 63.9(2), C1–Fe2–C6 36.7(2), Fe2–C1–C6 76.6(4), Fe2–C6–C1 66.8(3), Fe1–N1–N2 116.5(4), Fe2–N1–N2 124.7(4), C7–N1–N2 118.1(5), N1–N2–C8 117.6(5), N2–C8–C9 123.0(6).

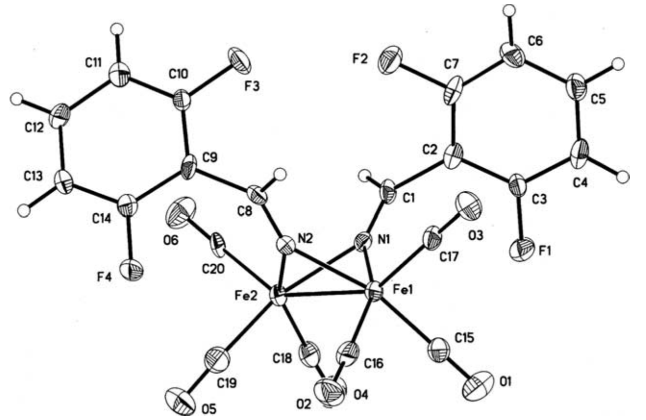

Fig. 4. Molecular structure of **4**. Selected bond lengths (pm) and angles (°): Fe1–Fe2 241.2(2), Fe1–N1 193.5(6), Fe1–N2 191.8(6), Fe2–N1 192.8(6), Fe2–N2 194.1(6), N1–C1 123.9(9), N2–C8 125.2(9), Fe1–Fe2–N1 51.5(2), Fe1–Fe2–N2 50.9(2), N1–Fe1–Fe2 51.2(2), N1–Fe1–N2 73.7(2), Fe1–N1–Fe2 77.3(2), Fe1–N2–Fe2 77.4(2), Fe1–N1–C1 140.9(5), Fe2–N1–C1 140.0(5), Fe1–N2–C9140.7(6), Fe2–N2–C9 138.9(6), N1–C1–C2 122.4(7), N2–C8–C9 122.7(7).

CH_2Cl_2 nor with ether, which was pre-dried over NaOH, as the solvent. But using ethanol **6** was obtained from the chromatography. So most probably ether is the source of the sodium cations as well as of the water present in the crystal structure. Cluster anions as in **6** were identified on the basis of spectroscopic evidence by Kaesz and coworkers as the intermediates in the reaction of carbonyl ferrates with moist nitriles [16a]. To the best of our knowledge this is the first time that these cluster anions are structurally characterized and thus may be compared to their derivatives of types **2** and **7** (vide infra).

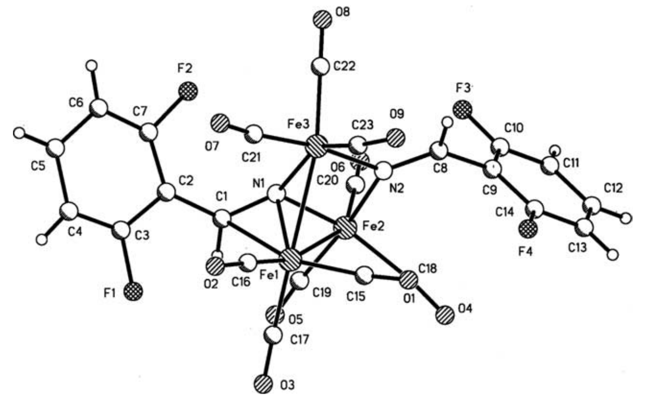

Fig. 5. Structural motif of **5**.

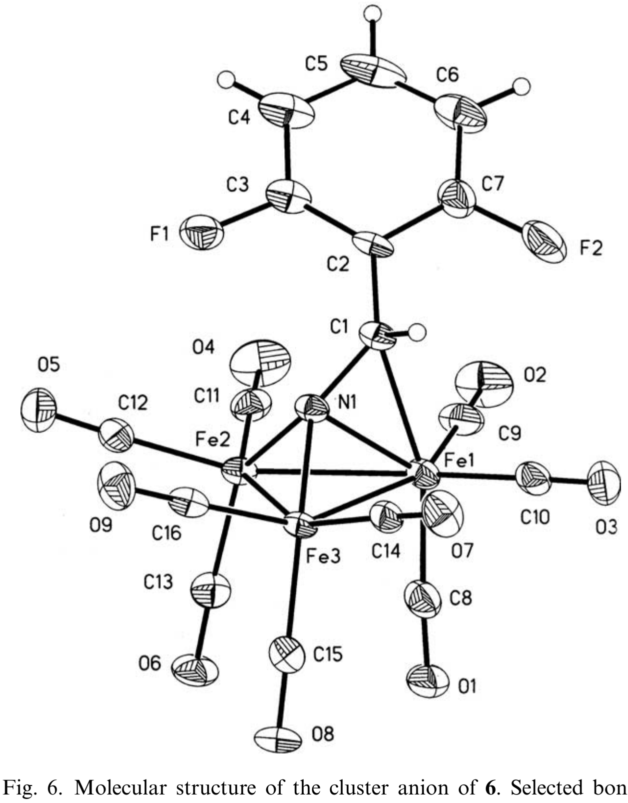

Fig. 6. Molecular structure of the cluster anion of **6**. Selected bond lengths (pm) and angles (°): Fe1–Fe2 255.2(1), Fe1–Fe3 254.51(9), Fe2–Fe3 251.22(9), Fe1–N1 195.4(4), Fe2–N1 185.4(4), Fe3–N1 185.7(3), Fe1–C1 218.4(4), C1–N1 133.6(5), C1–C2 149.4(6), Fe2–Fe1–Fe3 59.06(2), Fe1–Fe2–Fe3 60.34(3), Fe2–Fe3–Fe1 60.60(3), Fe2–Fe1–N1 46.3(1), Fe3–Fe1–N1 46.5(1), Fe1–Fe2–N1 49.6(1), Fe3–Fe2–N1 47.5(1), Fe1–Fe3–N1 49.8(1), Fe2–Fe3–N1 47.3(1), Fe1–N1–Fe2 84.1(1), Fe1–N1–Fe3 83.8(1), Fe2–N1–Fe3 85.2(1), C1–N1–Fe1 80.8(3), C1–N1–Fe2 137.1(3), C1–N1–Fe3 132.0(3), C1–Fe1–N1 37.2(2), C1–Fe1–Fe2 77.4(1), C1–Fe1–Fe3 76.0(1), Fe1–C1–N1 62.0(2), Fe1–C1–C2 119.7(3), N1–C1–C2 123.7(5). The bond lengths and angles of the second anion being present in the asymmetric unit of the crystal structure are identical within experimental errors.

The anion of **6** shows a trinuclear cluster core consisting of a Fe_3N tetrahedron with one of the FeN edges of the tetrahedron being bridged by the former imine carbon atom. So the anion may also be described as a formally six electron donating arylidenimido ligand coordinated to a triangular $Fe_3(CO)_9$ cluster fragment. The carbon nitrogen bond length of course is elongated due to the coordination towards the transition metal centers and is very similar to those observed for the closely related compounds **2a** and **2b**, respectively.

The crystal structure of **6** is shown in Fig. 7. The crystal packing is realized by the coordination of the two water molecules to sodium cations building up a four membered ring. Both sodium cations show a distorted octahedral coordination sphere being completed by interactions with carbon monoxide ligands of neighboring cluster anions. In addition, the water molecules each show two hydrogen bonding interactions with CO groups of cluster anions. On the right side of Fig. 7 the coordination mode of the sodium cations together with the hydrogen bridges is depicted.

It is has been pointed out before, that ionic compounds of type **6** have been postulated to be the intermediates in the reaction of carbonyl ferrates with nitriles in the presence of a proton source leading to the formation of tetrahedral cluster compounds of the composition $[Fe_3(CO)_9(\mu_2\text{-}H)(\mu_3\text{-}\eta^2\text{-}N{=}CHR)]$ [18]. Scheme 4 shows the reaction of **6** with phosphoric acid leading to the quantitative formation of **7**. In analogy to derivatives of **7** the molecular structure is closely related to **6** with the exception, that the iron iron bond between Fe2 and Fe3, which are not coordinated to arylidenamido ligand, now are bridged by a hydride ligand [15,16]. Fig. 8 shows the molecular structure of **7** together with the most interesting bond lengths and angles. The position of the hydride ligand

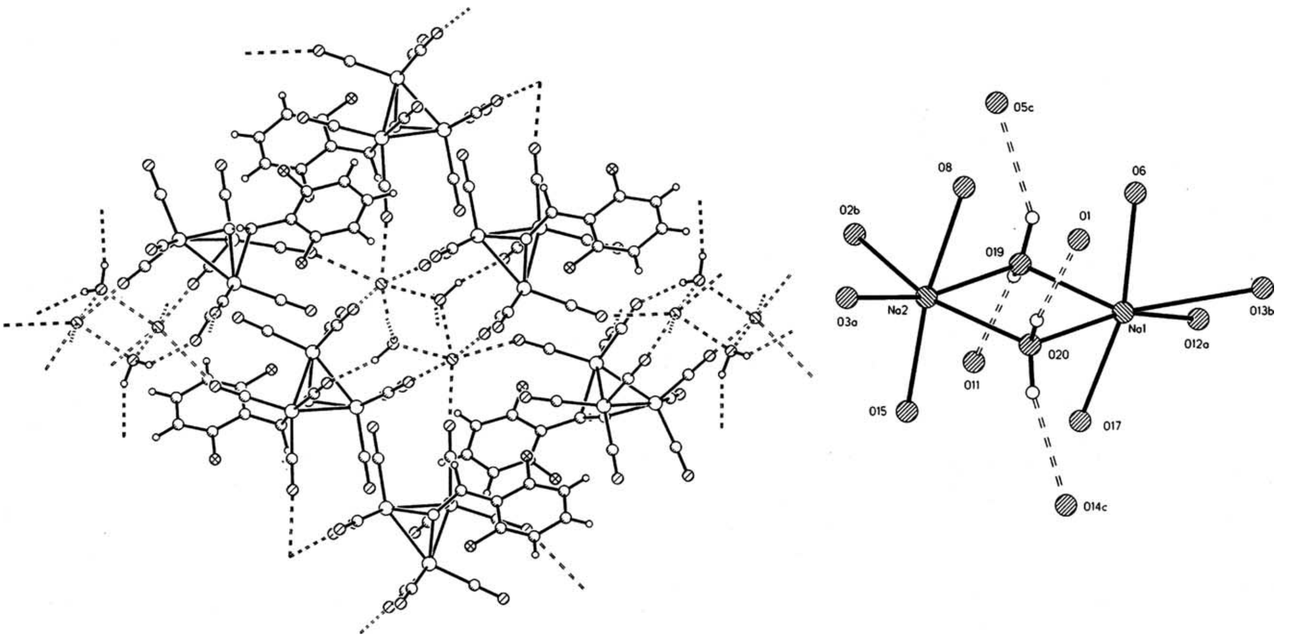

Fig. 7. Crystal structure of $[Fe_3(CO)_9(\mu_3\text{-}\eta^2\text{-}N{=}CHR)]Na \times H_2O$, **6**, showing the coordination sphere of the sodium cations built up by water molecules and CO ligands from neighboring cluster anions. Selected bond lengths (pm) and angles (°): Na1–O19 243.7(4), Na1–O20 241.5(5), Na2–O19 240.3(5), Na2–O20 244.4(4), Na1–O6 235.6(4), Na1–O12 242.4(4), Na1–O13 273.4(4), Na1–O17 241.2(3), Na2–O2 304.2(5), Na2–O3 244.4(4), Na2–O8 243.9(3), Na2–O15 235.4(4), O11–H19a 221(1), O5–H19b 224(1), O14–H20a 220(1), O1–H20b 218 (1), O19–Na1–O20 80.9(1), Na1–O20–Na2 98.8(2), O20–Na2–O19 81.0(1), Na2–O19–Na1 99.3(2).

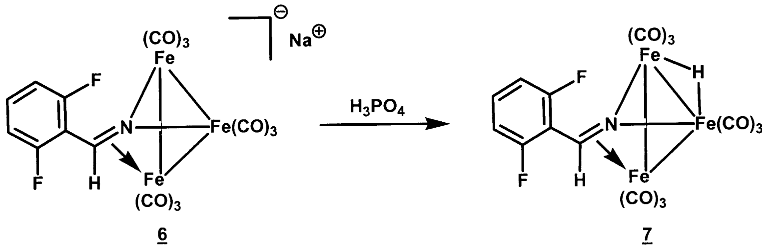

Scheme 4.

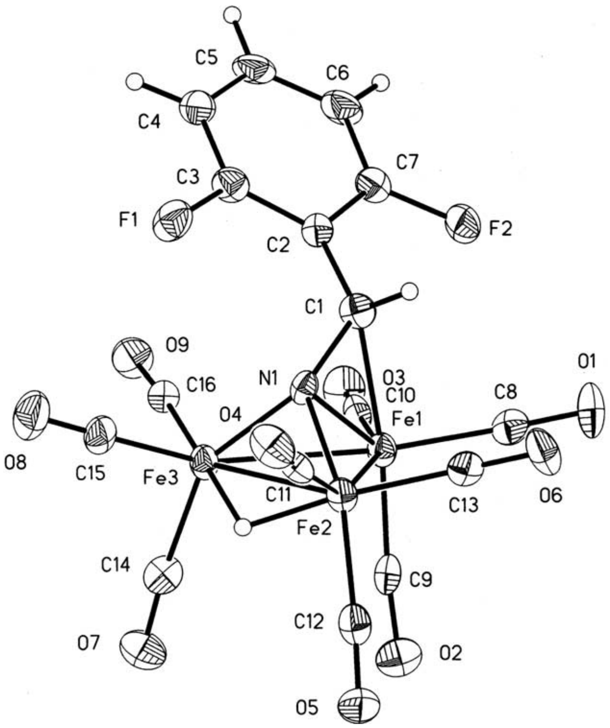

Fig. 8. Molecular structure of of **7**. Selected bond lengths (pm) and angles (°): Fe1–Fe2 254.3(2), Fe1–Fe3 256.1(2), Fe2–Fe3 258.9(2), Fe1–N1 194.8(8), Fe2–N1 188.3(7), Fe3–N1 185.1(8), Fe1–C1 218.6(9), C1–N1 134.8(9), C1–C2 149(1), Fe2–Fe1–Fe3 60.95(5), Fe1–Fe2–Fe3 59.87(5), Fe2–Fe3–Fe1 59.18(5), Fe2–Fe1–N1 47.3(2), Fe3–Fe1–N1 46.0(2), Fe1–Fe2–N1 49.5(2), Fe3–Fe2–N1 45.6(2), Fe1–Fe3–N1 49.2(2), Fe2–Fe3–N1 46.6(2), Fe1–N1–Fe2 83.2(3), Fe1–N1–Fe3 84.7(3), Fe2–N1–Fe3 87.8(3), C1–N1–Fe1 80.9(5), C1–N1–Fe2 128.9(6), C1–N1–Fe3 138.0(7), C1–Fe1–N1 37.5(3), C1–Fe1–Fe2 76.0(2), C1–Fe1–Fe3 77.7(2), Fe1–C1–N1 61.6(5), Fe1–C1–C2 117.6(7), N1–C1–C2 122.8(8).

was determined from the Difference Fourier map and was refined without any constraints.

The most significant differences in the bond lengths of **2a**, **2b**, **6** and **7** correspond to the iron iron bonds. In **6** Fe1–Fe2 and Fe1–Fe3 are nearly identical whereas the Fe2–Fe3 bond is about 3 pm shorter (251.22(9) pm). In contrast to this observation the corresponding Fe2–Fe3 bonds are longer in **7** (258.9(2) pm), in which this bond is bridged by a hydride ligand and **2a** and **2b** with a semi-bridging CO ligand (263.7(1) and 261.92(4) pm). In **2a** and **2b** also the Fe1–Fe2 bonds are elongated compared to **6** due to the coordination of the aromatic substituent to Fe2 after the activation of the corresponding carbon–halogen bonds (Figs. 1 and 2). The coordination of the nitrogen atoms of the arylideneamido ligand is nearly identical in all compounds. In **6** the iron nitrogen bond Fe1–N1 is app. 10 pm longer compared to Fe2–N1 and Fe3–N1. The reason for this is obviously the side-on coordination of the carbon nitrogen double bond to Fe1. The C1–N1 bond length measures to 133.6(5) pm. Significantly different are the C1–Fe1 bond lengths which are about 5 pm longer in **2a** and **2b** compared to **6** (218.4(4) pm) and **7**.

Kaesz and coworkers [18] showed that the synthesis of compounds of type **7** may be achieved by reacting the corresponding nitriles with carbonylferrates. The yield of **6**, from which we were able to produce **7** (Schemes 3 and 4), was very low. So we decided to react 2,6-difluorobenzonitrile with $Fe_2(CO)_9$ to produce larger quantities of **7**. The trinuclear iron carbonyl cluster compound **8** is however the sole product, that might be isolated from the reaction mixture after chromatographic workup (Scheme 5). Fig. 9 shows the molecular structure of **8** together with the most important bond lengths and angles. Compounds of type **8** have also been obtained and structurally characterized earlier from the reaction of $[HFe_3(CO)_{11}]^-$ with most nitriles in the presence of a proton source leading to $[Fe_3(CO)_9(\mu_2\text{-H})(\mu_3\text{-}\eta^2\text{-N{=}CHR})]$ as an intermediate, which produces $[Fe_3(CO)_9(\mu_3\text{-}\eta^2\text{-N}{\equiv}\text{CR})]$ by air oxidation [18]. In another reference a derivative of **8** was directly synthesized from $Fe_3(CO)_{12}$ and benzonitrile in the presence of a proton source [21]. The structural properties of **8** are essentially identical to the compounds reported in the literature. **8** is a trinuclear iron carbonyl cluster which is best described as a Fe_3N tetrahedron with one of the Fe_2N faces of the tetrahedron being capped by a carbon atom. So the nitrile ligand shows a μ_3-η^2-coordination to the iron triangle. The iron nitrogen bond length Fe1–N1 measures to 178.7(2) pm and is therefore significantly shorter as the other iron nitrogen bonds (195.9(2) and 196.2(2) pm). The bond lengths of C1 towards Fe2 and Fe3 are nearly identical and the carbon nitrogen bond of the nitrile ligand is slightly elongated to

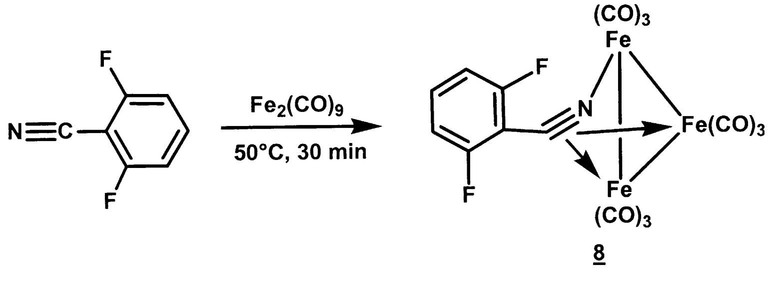

Scheme 5.

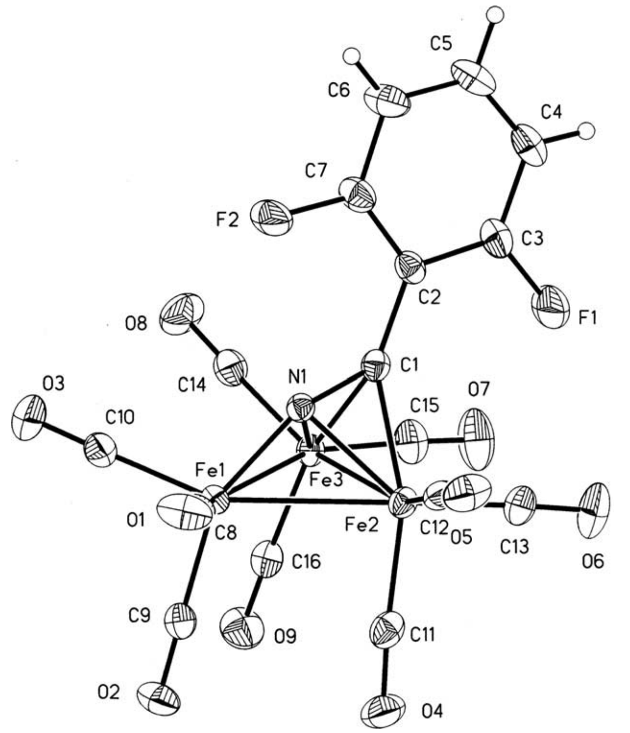

Fig. 9. Molecular structure of **8**. Selected bond lengths (pm) and angles (°): Fe1–Fe2 263.82(5), Fe1–Fe3 261.56(5), Fe2–Fe3 246.90(5), Fe1–N1 178.7(2), Fe2–N1 195.9(2), Fe3–N1 196.2(2), Fe2–C1 204.0(4), Fe3–C1 206.0(2), C1–N1 128.4(3), C1–C2 145.0(3), Fe2–Fe1–Fe3 56.06(1), Fe1–Fe2–Fe3 61.51(1), Fe2–Fe3–Fe1 62.43(1), Fe2–Fe1–N1 47.95(6), Fe3–Fe1–N1 48.58(6), Fe1–Fe2–N1 42.62(6), Fe3–Fe2–N1 51.03(6), Fe1–Fe3–N1 43.06(6), Fe2–Fe3–N1 50.92(6), Fe1–N1–Fe2 89.43(9), Fe1–N1–Fe3 88.36(9), Fe2–N1–Fe3 78.05(7), C1–N1–Fe1 159.33(2), C1–N1–Fe2 74.7(2), C1–N1–Fe3 75.6(1), C1–Fe2–N1 37.39(9), C1–Fe2–Fe3 53.35(7), C1–Fe2–Fe1 79.36(7), C1–Fe3–Fe1 79.57(7), C1–Fe3–Fe2 52.61(7), C1–Fe3–N1 37.14(9), Fe2–C1–Fe3 74.04(9), Fe2–C1–N1 67.9(1), Fe3–C1–N1 67.3(1), Fe2–C1–C2 144.6(2), Fe3–C1–C2 136.5(2), N1–C1–C2 133.1(2).

128.4(3) pm due to the triply bridging coordination mode. The iron iron bond that is bridged by the nitrile ligand (Fe2–Fe3) is *circa* 18 pm longer compared to the other two iron iron bonds.

In conclusion we were able to show that the reaction of aromatic aldazines with halogen substituents in the 2- and 6-positions with $Fe_2(CO)_9$ proceeds via two main pathways. The major pathway is the symmetrical cleavage of the central nitrogen nitrogen bond leading to the bis-(μ-iminato) compounds **4**. Addition of another $Fe(CO)_3$ moiety produces clusters of type **5**. The elimination of one of the iminato moieties leads to trinuclear ionic compounds of type **6**. In addition, we were able to isolate compounds in which one of the carbon halogen bonds in *ortho*-position with respect to the imine function is activated creating a new iron carbon bond. According to the nearly identical cluster cores in **6** and **2a** or **2b**, respectively, it might be suggested, that the latter are produced from **6** by the elimination of the corresponding halide. The minor pathway is represented by compound **3**, in which the azine ligand is still preserved. During the formation of **3** also one of the carbon fluorine bonds has been activated.

3. Experimental

3.1. General

All procedures were carried out under an argon atmosphere in anhydrous, freshly distilled solvents except the synthesis of **6**, in which neat diethylether has been used. Infrared spectra were recorded on a Perkin–Elmer FT-IR System 2000 using 0.2 mm KBr cuvettes. NMR spectra were recorded on a Bruker AC 200 spectrometer (^1H: 200 MHz, ^{13}C: 50.32 MHz, $CDCl_3$ as internal standard). Mass spectra were recorded on a Finnigan MAT SSQ 710 instrument. High resolution mass spectra (HRMS) were carried out using a Finnigan MAT 95 XL spectrometer using FAB techniques.

3.2. X-ray crystallographic studies

The structure determinations of **2a, 2b, 3–8** were carried out on an Enraf Nonius Kappa CCD diffractometer, crystal detector distance 25 mm, using graphite monochromated Mo Kα radiation. The crystal was mounted in a stream of cold nitrogen. Data were corrected for Lorentz and polarization effects but not for absorption. The structure was solved by direct methods and refined by full-matrix least squares techniques against F^2 using the programs SHELXS-86 and SHELXL-97 [22]. Computation of the structure was accomplished with the program XPMA [23] and the molecular illustration was drawn using the program XP [24]. The crystal and intensity data are given in Table 1.

Additional material on the structure analyses is available from the Cambridge Crystallographic Data Centre by mentioning the deposition number CCDC-228279 (**2a**), CCDC-228280 (**2b**), CCDC-228281 (**3**), CCDC-228282 (**4**), CCDC-228283 (**8**), CCDC-228284 (**6**), CCDC-228285 (**7**). The quality of the crystals of **5** was only sufficient to obtain a structural motif of the compound. The crystal and intensity data are therefore not given and were also not deposited at the CCDC.

3.3. Synthesis of *1a, 1b*

A 1 ml portion of hydrazine hydrate (20 mmol) was stirred together with an equimolar amount of the corresponding aldehyde (2.84 g, 2.16 ml difluorobenzaldehyde;

3.5 g dichlorobenzaldehyde) in 50 ml ethanol. After precipitation of the product it was washed twice with cold ethanol to yield 5.09 g (74%) **1a** or 4.59 g (82%) **1b**, respectively, as analytically pure yellow crystalline material. **1a** was identified by its melting point, which was identical to the one reported in the literature [25].

3.4. MS and spectroscopical data for **1a**

HRMS calcd. for $C_{14}H_8N_2NaCl_4$ (MNa^+) 366.9341. Found 366.9339, $\Delta = 0.19$ mmu. MS (EI): *m/z* (%) 344 (M^+, 7), 309 ($M^+ - Cl$, 100), 276 ($M^+ - 2Cl$, 69), 239 ($M^+ - 3Cl$, 5), 172 ($C_7H_4NCl_2^+$, 5), 145 ($C_6H_3Cl_2^+$, 4), 136 ($C_7H_3NCl^+$, 8), 123 ($C_7H_4Cl^+$, 7), 109 ($C_6H_2Cl^+$, 5), 100 ($C_7H_2N^+$, 5), 75 ($C_6H_3^+$, 4). IR (KBr, cm^{-1}): 1625 s, 1581 s, 1557 s, 1428 s, 1331 s, 1267 m, 1215 m, 1190 s, 1151 m, 1093 m, 969 w, 948 m, 897 w, 873 s, 777 vs, 728 s, 679 s, 533 w, 514 w, 456 s, 402 s. ^1H NMR (200 MHz, $CDCl_3$, 298 K): 7.17–7.36 (m, 3H, $^3J_{HH} = 8.7$ Hz), 8.76 (s, 1H). ^{13}C NMR (50.3 MHz, $CDCl_3$, 298 K): 128.94, 130.21, 130.99, 135.51, 157.61.

3.5. MS and spectroscopical data for **1b**

HRMS calcd. for $C_{14}H_9N_2F_4$ (MH^+) 281.0704. Found 281.0702, $\Delta = 0.17$ mmu. MS (EI): *m/z* (%) 280 (M^+, 100), 261 ($M^+ - F$, 36), 153 ($C_8H_5NF_2^+$, 23), 140 ($C_7H_4NF_2^+$, 48), 126 ($C_7H_4F_2^+$, 20), 120 ($C_7H_3NF^+$, 43), 113 ($C_6H_3F_2^+$, 14), 100 ($C_7H_2N^+$, 11), 63 ($C_5H_3^+$, 18). IR (KBr, cm^{-1}): 3092 w, 1625 s, 1584 s, 1579 s, 1562 s, 1477 s, 1458 s, 1336 s, 1298 m, 1273 m, 1244 s, 1212 s, 1157 m, 1015 s, 971 m, 956 m, 879 w, 851 s, 785 s, 717 s, 610 s, 533 s, 517, w, 506 m, 424 w. ^1H NMR (400 MHz, $CDCl_3$, 298 K): 6.98 (dd, 2H, $^3J_{HH} = 8.4$ Hz, $^3J_{HF} = 8.7$ Hz), 7.39 (tt, 1H, $^4J_{HF} = 6.2$ Hz, $^3J_{HH} = 8.4$ Hz), 8.87 (s, 1H). ^{13}C NMR (100.6 MHz, $CDCl_3$, 298 K): 111.7 (t, $^2J_{CF} = 13$ Hz), 112.12 (d, $^2J_{CF} = 25$ Hz), 132.54 (t, $^3J_{CF} = 11$ Hz), 153.69 (s), 161.86 (dd, $^1J_{CF} = 259$ Hz, $^3J_{CF} = 6$ Hz).

3.6. Synthesis of **2a**, **2b**, **3**–**6**

A 360 mg portion $Fe_2(CO)_9$ (1 mmol) together with an equimolar amount of the corresponding azine (280 mg **1a**, 310 mg **1b**) and 20 ml *n*-heptane are stirred together at 50 °C for 45 min. In the course of the reaction the pale yellow suspension slowly changes to a deep red solution as the ligand and $Fe_2(CO)_9$ dissolve. After the reaction is completed all volatile materials are removed in vacuo. The residue is dissolved in CH_2Cl_2, 1 g silanized silica gel is added and the solvent is again removed under reduced pressure. Chromatography on silica gel using light petroleum (b.p. 40–60 °C) as the eluent first yields a green band containing $Fe_3(CO)_{12}$ followed by a dark brown band of **2a** or **2b,** respectively. Adding small portions of CH_2Cl_2 to the light petroleum allows the elution of the iron carbonyl compounds **3**–**6.** The bis-(μ-iminato) complexes **4** and **5** are obtained with a light petroleum CH_2Cl_2 ratio of 40:1. Increasing the amount of CH_2Cl_2 to 10:1 leads to the elution of a red band containing **3**. Using CH_2Cl_2/ether 1:1 as the solvent leads to the elution of unconverted **1b**. The ionic compound **6** may be eluted with ethanol as the solvent only if the column was washed with ether (pre-dried over NaOH) in advance. Yields (based on the portion of the converted azines): 2 mg **2a** (0.003 mmol, 1%), 6 mg **2b** (0.01 mmol, 3%), 2 mg **3** (0.004 mmol, 1%), 12 mg **4**, (0.02 mmol, 7%), 10 mg **5** (0.01 mmol, 5%), 7 mg **6** (0.01 mmol, 4%). Due to the very low yields of **2a**, **2b** and **3** and the poor solubility of **6** ^{13}C NMR spectra could not be obtained for these compounds and HRMS could not be determined for **3** and **6**. Nevertheless, the molecular structure of these complexes was unequivocally demonstrated by X-ray analyses. Recrystallization of the complexes was performed from mixtures of light petroleum (b.p. 40–60 °C) and CH_2Cl_2 at −20 °C for **2a**, **2b**, **3**–**5**. **6** was recrystallized from an ethanolic solution carefully underlayered with CH_2Cl_2 at room temperature. Only one single crystal of **2a** was obtained after the chromatographic work up procedure which proved sufficient to carry out a crystallographic analysis but prevented a thorough spectroscopic characterization of the cluster. Since crystalline **6** is not soluble in common solvents it was not possible to obtain NMR spectra.

3.7. MS and spectroscopical data for **2b**

The compound is too volatile to obtain a HRMS spectrum. $C_{16}H_4NFO_9Fe_3$ MS (EI): *m/z* (%) 541 (M^+, 6), 513 ($M^+ - CO$, 53), 485 ($M^+ - 2CO$, 100), 457 ($M^+ - 3CO$, 22), 429 ($M^+ - 4CO$, 39), 401 ($M^+ - 5CO$, 72), 373 ($M^+ - 6CO$, 65), 345 ($M^+ - 7CO$, 42), 317 ($M^+ - 8CO$, 42), 289 ($M^+ - 9CO$, 35), 233 ($C_7H_4NFFe_2^+$, 16), 196 ($C_7H_4NF_2Fe^+$, 16), 168 (Fe_3^+, 15), 112 (Fe_2^+, 24), 84 ($FeCO^+$,13), 56 (Fe^+, 15). IR (KBr, cm^{-1}): 2085 s, 2051 s, 2044 s, 2032 s, 2021 s, 2008 s, 2001 s, 1995 s, 1977 s, 1966 m, 1949 s, 1631 m, 1591 w, 1464 w, 1262 m, 1230 w, 1106 m, 1021 m, 856 w, 802 m, 776 m, 742 w, 620 w, 594 w, 553 m, 535 w. ^1H {^{19}F} NMR (200 MHz, CD_2Cl_2, 298 K): 6.71 (d, 1H, $^3J_{HH} = 8.3$ Hz), 6 93 (dd, 1H, $^3J_{HH} = 8.3$ Hz, $^3J_{HH} = 7.5$ Hz), 7.42 (d, 1H, $^3J_{HH} = 7.5$ Hz), 8.02 (s, 1H). ^1H NMR (200 MHz, CD_2Cl_2, 298 K): 6.71 (dd, 1H,$^3J_{HH} = 8.3$ Hz, $^3J_{HF} = 9.8$ Hz), 6.93 (ddd, 1H, $^3J_{HH} = 8.3$ Hz, $^3J_{HH} = 7.5$ Hz, $^4J_{HF} = 5.4$ Hz), 7.42 (d, 1H, $^3J_{HH} = 7.5$ Hz), 8.02 (s, 1H).

3.8. MS and spectroscopical data for **3**

HRMS calcd. for $C_{20}H_9N_2F_3O_6Fe_2$ 541.9121. Found 541.9130, $\Delta = 0.99$ mmu. MS (EI): *m/z* (%) 542 (M^+, 10), 514 ($M^+ - CO$, 18), 486 ($M^+ - 2CO$, 60), 458

(M^+-3CO, 37), 430 (M^+-4CO, 25), 402 (M^+-5CO, 89), 374 (M^+-6CO, 100), 280 ($C_{10}H_4NF_20_3Fe^+$, 47), 261 ($C_{10}H_4NFO_3Fe^+$, 28), 251 ($C_7H_3NF_2Fe_2{}^+$, 18), 140 ($FeC_3O_3{}^+$, 36), 112 ($Fe_2{}^+$, 20). IR (KBr, cm^{-1}): 2074 s, 2031 s, 2005 s, 1983 sh, 1976 s, 1959 s, 1624 m, 1459 w, 1263 m, 1238 m, 1098 s, 1013 s, 805 s, 779 m, 626 w, 596 w, 569 w, 551 w. $^1H\ \{^{19}F\}$ NMR (200 MHz, CD_2Cl_2, 298 K): 4.41 (s, 1H), 6.97 (d, 2H, $^3J_{HH}=8.5$ Hz), 6.98 (d, 1H, $^3J_{HH}=8.0$ Hz), 7.15 (dd, 1H, $^3J_{HH}=8.0$ Hz, $^3J_{HH}=7.8$ Hz), 7.37 (t, 1H, $^3J_{HH}=8.5$ Hz) 7.85 (d, 1H, $^3J_{HH}=7.8$ Hz), 7.97 (s, 1H). ^1H NMR (200 MHz, CD_2Cl_2, 298 K): 4.41 (s, 1H), 6.97 (dd, 2H, $^3J_{HH}=8.5$ Hz, $^3J_{HF}=8.6$ Hz), 6.98 (dd, 1H, $^3J_{HH}=8.0$ Hz, $^3J_{HF}=9.1$ Hz), 7.15 (m, 1H, $^3J_{HH}=8.0$ Hz, $^3J_{HH}=7.8$ Hz, $^4J_{HF}=6.3$ Hz), 7.37 (tt, 1H, $^3J_{HH}=8.5$ Hz, $^4J_{HF}=6.3$ Hz) 7.85 (d, 1H, $^3J_{HH}=7.8$ Hz), 8.02 (s, 1H).

*3.9. MS and spectroscopical data for **4***

HRMS calcd. for $C_{20}H_8N_2F_4O_6Fe_2$ 559.9010. Found 559.9017, $\Delta=0.68$ mmu. MS (EI): *m/z* (%) 560 (M^+, 2), 532 (M^+-CO, 8), 504 (M^+-2CO, 5), 476 (M^+-3CO, 27), 448 (M^+-4CO, 11), 420 (M^+-5CO, 18), 392 (M^+-6CO, 100), 316 ($C_{14}H_7N_2F_3Fe^+$, 17), 271 ($C_7H_4NF_3Fe^+$, 71), 251 ($C_7H_3NF_2Fe_2{}^+$, 41), 244 ($C_6H_3F_3Fe_2{}^+$, 20), 196 ($C_7H_4NF_2Fe^+$, 52), 177 ($C_7H_4NFFe^+$,18), 150 ($Fe_2F_2{}^+$, 69), 132 ($HF_2Fe_2{}^+$, 92), 112 ($Fe_2{}^+$, 20), 75 (FeF^+, 66), 56 (Fe^+, 35). IR (KBr, cm^{-1}): 2924 m, 2076 s, 2037 s, 2004 sh, 1993 vs, 1976 s, 1969 s, 1624 m, 1465 s, 1008 m, 791 m, 762 m, 618 m, 573 m. $^1H\{^{19}F\}$ NMR (200 MHz, $CDCl_3$, 298 K): 6.93 (d, 2H, $^3J_{HH}=8.4$ Hz), 7.34 (t, 1H, $^3J_{HH}=8.4$ Hz), 8.74 (s, 1H). ^{13}C NMR (100.6 MHz, $CDCl_3$, 298 K): 111.70 (m, $^2J_{CF}=19$ Hz, $^4J_{CF}=5$ Hz), 117.58 (t, $^2J_{CF}=20$ Hz), 131.02 (t, $^3J_{CF}=10$ Hz), 159.28 (d of d, $^1J_{CF}=250$ Hz, $^3J_{CF}=7$ Hz), 163.66 (s), no CO resonances observed at room temperature.

*3.10. MS and spectroscopical data for **5***

HRMS calcd. for $C_{23}H_8N_2F_4O_9Fe_3$ 699.8218. Found 699.8222, $\Delta=0.40$ mmu. MS (FAB): *m/z* (%) 700 (M^+, 3), 672 (M^+-CO, 15), 644 (M^+-2CO, 11), 616 (M^+-3CO, 47), 588 (M^+-4CO, 4), 560 (M^+-5CO, 6), 532 (M^+-6CO, 43), 504 (M^+-7CO, 24), 476 (M^+-8CO, 100), 448 (M^+-9CO, 26), 252 ($C_7H_4NF_2Fe_2{}^+$, 55), 233 ($C_7H_4NFFe_2{}^+$, 34), 206 ($C_8H_3O_2FFe^+$, 24), 188 ($C_8H_4O_2Fe^+$, 14), 150 ($Fe_2F_2{}^+$, 14), 132 ($HF_2Fe_2{}^+$, 23), 112 ($Fe_2{}^+$, 22), 75 (FeF^+, 8), 56 (Fe^+, 16). IR (KBr, cm^{-1}): 2923 m, 2080 w, 2049 s, 2025 s, 2000 s, 1990 sh, 1982 sh, 1974 sh, 1963 w, 1646 sh, 1624 m, 1465 m, 1236 w, 1006 m, 784 m, 766 w, 649 m, 616 m, 561 m. $^1H\{^{19}F\}$ NMR (200 MHz, $CDCl_3$, 298 K, mixture of *syn*- and *anti*-isomers): 6.55 (s, 0.4H), 7.01 (s, 0.6H), 7.01 (d, 2.4H, $^3J_{HH}=8.4$ Hz), 7.03 (d, 1.6H, $^3J_{HH}=7.9$ Hz), 7.34 (t, 0.4H, $^3J_{HH}=7.6$ Hz), 7.36 (t, 0.6H, $^3J_{HH}=8.4$ Hz), 7.44 (t, 0.4H, $^3J_{HH}=8.3$ Hz), 7.46 (t, 0.6H, $^3J_{HH}=8.5$ Hz), 8.62 (s, 1H). ^{13}C NMR (50.3 MHz, $CDCl_3$, 298 K, mixture of *syn*- and *anti*-isomers): 107.80 (s), 108.13 (s), 111.81 (m), 117.75 (m, $^2J_{CF}=22$ Hz), 120.64 (t, $^2J_{CF}=17$ Hz), 130.56 (t, $^3J_{CF}=10$ Hz), 131.62 (t, $^3J_{CF}=10$ Hz), 159.03 (d of d, $^1J_{CF}=250$ Hz, $^3J_{CF}=7$ Hz), 159.09 (d of d, $^1J_{CF}=250$ Hz, $^3J_{CF}=7$ Hz), 166.86 (s), 203.56 (s), 204.15 (s), 204.75 (s), 205.08 (s), 205.34 (s), 208.40 (s), 208.90 (s), 211.09 (s), 211.75 (s), 212.76 (s, broad).

*3.11. MS and spectroscopical data for **6***

$C_{16}H_4NF_2O_9Fe_3Na\times H_2O$; MS (EI): *m/z* (%) 504 ($C_{16}H_4NF_2O_9Fe_3{}^+$–2CO, 1), 476 ($C_{16}H_4NF_2O_9Fe_3{}^+$–3CO, 1), 448 ($C_{16}H_4NF_2O_9Fe_3{}^+$–4CO, 1), 420 ($C_{16}H_4NF_2O_9Fe_3{}^+$–5CO, 1), 392 ($C_{16}H_4NF_2O_9Fe_3{}^+$–6CO, 1), 364 ($C_{16}H_4NF_2O_9Fe_3{}^+$–7CO, 1), 336 ($C_{16}H_4NF_2O_9Fe_3{}^+$–8CO, 1), 308 ($C_{16}H_4NF_2O_9Fe_3{}^+$–9CO, 1), 280 ($C_8H_4NF_2OFe_2{}^+$, 1), 252 ($C_7H_4NF_2Fe_2{}^+$, 1), 139 ($C_7H_3NF_2{}^+$, 100). IR (KBr, cm^{-1}): 2924 m, 2074 s, 2035 vs, 1999 sh, 1991 s, 1978 s, 1624 m, 1465 m, 1007 m, 788 m, 580 m.

3.12. Synthesis of 7

A 10 mg sample of **6** was dissolved in 85% phosphoric acid. Extraction of the crude reaction mixture with light petroleum (b.p. 40–60 °C) followed by chromatographic workup using a mixture of light petroleum and CH_2Cl_2 5:1 yields 8 mg (85%) of **7**. Recrystallization of **7** was performed from mixtures of light petroleum (b.p. 40–60 °C) and CH_2Cl_2 at −20 °C.

3.13. MS and spectroscopical data of 7

HRMS calcd. for $C_{16}H_5NF_2O_9Fe_3$ 560.7976. Found 560.7971, $\Delta=0.48$ mmu. MS (EI): *m/z* (%) 561 (M^+, 10), 533 (M^+-CO, 6), 505 (M^+-2CO, 17), 477 (M^+-3CO, 6), 449 (M^+-4CO, 8), 421 (M^+-5CO, 75), 393 (M^+-6CO, 43), 365 (M^+-7CO, 43), 337 (M^+-8CO, 100), 309 (M^+-9CO, 50), 251 ($C_7H_3NF_2Fe_2{}^+$, 30), 233 ($C_7H_4NFFe_2{}^+$, 16), 213 ($C_7H_4NFe_2{}^+$, 33), 196 ($C_7H_4NF_2Fe^+$, 24), 188 ($HFFe_3{}^+$, 44), 169 ($HFe_3{}^+$, 30), 168 ($Fe_3{}^+$, 30), 132 ($HF_2Fe_2{}^+$, 68), 112 ($Fe_2{}^+$, 77), 75 (FeF^+, 18), 56 (Fe^+, 55).

*3.14. Synthesis of **8***

A 360 mg portion $Fe_2(CO)_9$ (1 mmol) together with a five fold excess of 2,6-difluorobenzonitrile (695 mg, 0.56 ml) was stirred in 20 ml *n*-heptane at 50 °C for 2 h.

During the reaction time the solution turned deep green as the iron carbonyl dissolves. After the reaction is completed all volatile materials are removed in vacuo.

The residue is dissolved in CH_2Cl_2, 1 g silanized silica gel is added and the solvent is again removed under reduced pressure. Chromatography on silica gel using light petroleum (b.p. 40–60 °C) as the eluent first yields a green band containing $Fe_3(CO)_{12}$ followed by a dark brown band of **8** if a mixture of ight petroleum and CH_2Cl_2 20:1 is used as the eluent. Unfortunately, unconverted nitrile elutes together with **8**. Recrystallization of **8** from mixtures of light petroleum (b.p. 40–60 °C) and CH_2Cl_2 at −20 °C yields two types of crystals: colourless plates of 2,6-difluorobenzonitrile and black prisms of **8**. Yield (based on $Fe_2(CO)_9$): 15 mg (0.03 mmol, 3%).

*3.15. MS and spectroscopical data of **8***

HRMS calcd. for $C_{16}H_3NF_2O_9Fe_3$ 558.7822. Found 558.7820, $\Delta = 0.17$ mmu. MS (El): m/z (%) 559 (M^+, 16), 531 ($M^+ - CO$, 10), 503 ($M^+ - 2CO$, 28), 475 ($M^+ - 3CO$, 4), 447 ($M^+ - 4CO$, 6), 419 ($M^+ - 5CO$, 100), 391 ($M^+ - 6CO$, 28), 363 ($M^+ - 7CO$, 22), 335 ($M^+ - 8CO$, 25), 307 ($M^+ - 9CO$, 31), 251 ($M^+ - Fe$–9CO, 23), 213 ($M^+ - FeF_2$–9CO, 13), 195 ($M^+ - 2Fe$–9CO, 5), 168 ($FeC_4O_4^+$, 23), 139 ($C_7H_3NF_2^+$, 48), 112 ($FeC_4O_4^+$, 23), 84 ($FeCO^+$, 8), 75 (FeF^+, 11), 56 (Fe^+, 37). IR (KBr, cm^{-1}): 2089 s, 2058 s, 2046 sh, 2029 s, 2016 s, 2004 sh, 1985 s, 1970 s, 1965 s, 1621 w, 1596 w, 1583 w, 1470 m, 1263 w, 1243w, 1190 w, 1100 w, 1011 m, 848 w, 789 m, 710 w, 604 m, 577 m, 558m, 530 w. ^{1}H NMR (200 MHz, $CDCl_3$, 298 K): 7.13 (d of d, 2H, $^3J_{HF} = 7.5$ Hz, $^3J_{HH} = 8.5$ Hz), 7.51 (t of t, 1H, $^4J_{HF} = 6.3$ Hz, $^3J_{HH} = 8.5$ Hz). ^{13}C NMR (100.6 MHz, $CDCl_3$, 298 K): 109.56 (t, $^2J_{CF} = 16$ Hz), 112.45 (d of d, $^2J_{CF} = 20$ Hz, $^4J_{CF} = 4$ Hz), 116.44 (s), 132.72 (t, $^3J_{CF} = 10$ Hz), 161.80 (d of d, $^1J_{CF} = 257$ Hz, $^3J_{CF} = 5$ Hz) 208.70 (s, broad).

References

[1] (a) J. Burdeniuc, B. Jedlicka, R.H. Crabtree, Chem. Ber. 130 (1997) 145;
(b) L. Kiplinger, T.G. Richmond, C.E. Osterberg, Chem. Rev. 94 (1994) 373;
(c) E.F. Murphy, R. Murugavel, H.W. Roesky, Chem. Rev. 97 (1997) 3425;
(d) T.G. Richmond, in: S. Murai (Ed.), Topics in Organometallic Chemistry, vol. 3, Springer, New York, 1999, p. 243;
(e) T. Braun, R.N. Perutz, J. Chem. Soc., Chem. Commun. (2003) 2749.

[2] (a) R.E. Banks, B.E. Smart, J.C. Tatlow (Eds.), Organoflurine Chemistry: Principles and Commercial Applications, Plenum, New York, 1994;
(b) T. Hiyama, Organofluorine Compounds, Springer, Berlin, 2000.

[3] (a) M.W. Bouwkamp, J. de Wolf, l.d.H. Morales, J. Germaca, A. Meetsma, S.I. Trojanov, B. Hessen, J.H. Teuben, J. Am. Chem. Soc. 124 (2002) 12956;
(b) B.M. Kraft, W.D. Jones, J. Organomet. Chem. 658 (2002) 132;
(c) P.E. O'Connor, D.J. Berg, T. Barclay, Organometallics 21 (2002) 3947;
(d) B.M. Kraft, R.J. Lachicotte, W.D. Jones, J. Am. Chem. Soc. 123 (2001) 10973;
(e) W.D. Jones, J. Chem. Soc., Dalton Trans. (2003) 3991.

[4] P. Barrio, R. Castarlenas, M.A. Estruelas, A. Lledos, F. Maseras, E. Onate, J. Tomas, Organometallics 20 (2001) 442.

[5] (a) L. Cronin, C.L. Higgitt, R. Karch, R.N. Perutz, Organometallics 16 (1997) 4920;
(b) T. Braun, S.P. Foxon, R.N. Perutz, P.H. Walton, Angew. Chem. 111 (1999) 3543;
(c) S.J. Archibald, T. Braun, J.F. Gaunt, J.E. Hobson, R.N. Perutz, J. Chem. Soc., Dalton Trans. (2000) 2013;
(d) T. Braun, L. Cronin, C.L. Higgitt, J.E. McGrady, R.N. Perutz, M. Reinhold, New J. Chem. 25 (2001) 19;
(e) M.I. Sladek, T. Braun, B. Neumann, H.-G. Stammler, J. Chem. Soc., Dalton Trans. (2002) 297;
(f) T. Braun, R.N. Perutz, M.I. Sladek, J. Chem. Soc., Chem. Commun. (2001) 2254.

[6] (a) D. Noveski, T. Braun, M. Schulte, B. Neumann, H.-G. Stammler, J. Chem. Soc., Dalton Trans. (2003) 4075;
(b) T. Braun, D. Noveski, B. Neumann, H.-G. Stammler, Angew. Chem. 114 (2002) 2870;
(c) M. Rausch, D. Steinborn, J. Organomet. Chem. 622 (1–2) (2001) 172;
(d) R. Bosque, E. Clot, S. Fantacci, F. Maseras, O. Eisenstein, R.N. Perutz, K.B. Renkema, K.G. Caulton, J. Am. Chem. Soc. 120 (1998) 12634;
(e) R.P. Hughes, D.C. Lindner, A.L. Rheingold, G.P.A. Yap, Organometallics 15 (1996) 5678;
(f) D. Noveski, T. Braun, M. Schulte, B. Neumann, H.-G. Stammler, J. Chem. Soc., Dalton Trans. (2003) 4075.

[7] (a) N.A. Jasim, R.N. Perutz, J. Am. Chem. Soc. 122 (2000) 8685;
(b) M.W. Holtcamp, J.A. Labinger, J.E. Bercaw, J. Am. Chem. Soc. 119 (1997) 848;
(c) M.W. Holtcamp, L.M. Henling, M.W. Day, J.A. Labinger, J.E. Bercaw, Inorg. Chim. Acta 270 (1998) 467.

[8] (a) F. Godoy, C.L. Higgitt, A.H. Klahn, B. Oelckers, S. Parsons, R.N. Perutz, J. Chem. Soc., Dalton Trans. (1999) 2039;
(b) A.H. Klahn, B. Oelckers, F. Godoy, M.T. Garland, A. Vega, R.N. Perutz, C.L. Higgitt, J. Chem. Soc., Dalton Trans. (1998) 3079.

[9] T.T. Tsou, J.K. Kochi, J. Am. Chem. Soc. 101 (1979) 6319.

[10] I. Bach, K.-R. Pörschke, R. Goddard, C. Kopiske, C. Krüger, A. Rufinska, K. Seevogel, Organometallics 15 (1996) 4959.

[11] M. Aizenberg, D. Milstein, J. Am. Chem. Soc. 117 (1995) 8674.

[12] (a) G. Wohlfarth, in: R. Banerjee (Ed.), Chemistry and Biochemistry of B_{12}, Wiley, New York, 1999 Chapter 35;
(b) U.E. Krone, R.K. Thauer, H.P.C. Hogenkamp, K. Steinbach, Biochemistry 30 (1991) 2713.

[13] (a) W. Imhof, J. Organomet. Chem. 533 (1997) 31;
(b) W. Imhof, Inorg. Chim. Acta 282 (1998) 111;
(c) W. Imhof, A. Göbel, D. Ohlmann, J. Flemming, H. Fritzsche, J. Organomet. Chem. 584 (1999) 33;
(d) W. Imhof, Organometallics 18 (1999) 4845;
(e) W. Imhof, A. Göbel, J. Organomet. Chem. 610 (2000) 102;
(f) A. Göbel, G. Leibeling, M. Rudolph, W. Imhof, Organometallics 22 (2003) 759.

[14] (a) D. Berger, W. Imhof, J. Chem. Soc., Chem. Commun. (1999) 1457;
(b) D. Berger, W. Imhof, Tetrahedron 56 (2000) 2015;
(c) W. Imhof, D. Berger, M. Kotteritzsch, M. Rost, B. Schönecker, Adv. Synth. Catal. 343 (2001) 795;
(d) D. Dönnecke, W. Imhof, Tetrahedron 59 (2003) 8499.

[15] D. Dönnecke, J. Wunderle, W. Imhof, J. Organomet. Chem. 689 (2004) 585.

[16] (a) R. Rumin, F.Y. Petillon, L. Manojlovic-Muir, K.W. Muir, D.S. Yufit, J. Chem. Soc., Chem. Commun. (1995) 1431;
(b) R. Rumin, K. Guennou, F.Y. Petillon, K.W. Muir, J. Chem. Soc., Dalton Trans. (1997) 1381;
(c) R. Rumin, K. Guennou, R. Pichon, F.Y. Petillon, K.W. Muir, D.S. Yufit, J. Organomet. Chem. 533 (1997) 177;
(d) K. Guennou-de Cadenet, R. Rumin, F.Y. Petillon, K.W. Muir, Organometallics 19 (2000) 1912;
(e) K. Guennou-de Cadenet, R. Rumin, F.Y. Petillon, D.S. Yufit, K.W. Muir, Eur. J. Inorg. Chem. (2002) 639.

[17] N.S. Martin, M. Catriona, M. Sloan, J. Organomet. Chem. 96 (1975) 383.

[18] (a) M.A. Andrews, H.D. Kaesz, J. Am. Chem. Soc. 101 (1979) 7238;
(b) M.A. Andrews, G. Van Buskirk, C.B. Knobler, H.D. Kaesz, J. Am. Chem. Soc. 101 (1979) 7245;
(c) M.A. Andrews, H.D. Kaesz, J. Am. Chem. Soc. 101 (1979) 7255;
(d) M.A. Andrews, C.B. Knobler, H.D. Kaesz, J. Am. Chem. Soc. 101 (1979) 7260.

[19] R. Cohen, B. Rybtchinski, M. Gandelmann, L.J.W. Shimon, J.M.L. Martin, D. Milstein, Angew. Chem. 115 (2003) 1993.

[20] (a) D. Bright, O.S. Mills, J. Chem. Soc., Chem. Commun. (1967) 245;
(b) M. Kilner, C. Midcaft, J. Chem. Soc., Chem. Commun. (1974) 1620;
(c) R.B. King, W.M. Douglas, Inorg. Chem. 13 (1974) 1339;
(d) A. Zimniak, Pol. J. Chem. 66 (1992) 1051;
(e) G. Gervasio, P.L. Stanghellini, R. Rosetti, Acta Crystallogr. B 37 (1987) 1198;
(f) A. Zimniak, Z. Buczkowski, Bull. Acad. Pol. Chim. 29 (1981) 231;
(g) Y. Chauvin, D. Commereuc, D. Hugo, A. de Cian, R. Weiss, New J. Chem. 3 (1979) 183.

[21] E. Keller, D. Wolters, Chem. Ber. 117 (1984) 1572.

[22] (a) G. Sheldrick, SHELXS-86, Universität Göttingen, 1986;
(b) G. Sheldrick, SHELXL-97, Universität Göttingen, 1997.

[23] L. Zsolnai, G. Huttner, XPMA, Universität Heidelberg, 1996.

[24] Siemens Analytical X-ray Inst. Inc., XP – Interactive Molecular Graphics, Vers. 4.2, 1990.

[25] V.G. Nenajdenko, A.V. Shastin, V.N. Korotchenko, N. Vasily, G.N. Vaseev, E.S. Balenkowa, Eur. J. Org. Chem. (2003) 302.